

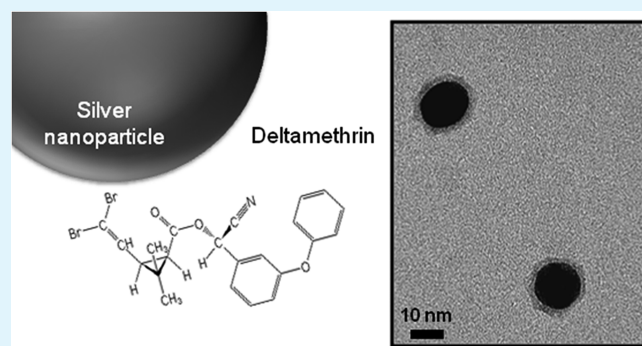
Surface Functionalization of Silver Nanoparticles: Novel Applications for Insect Vector Control

Aishwarya Sooresh,[†] Hyeogsun Kwon,[‡] Robert Taylor,[§] Patricia Pietrantonio,[‡] Michelle Pine,^{*,§} and Christie M. Sayes^{*,†,⊥}

[†]Interdisciplinary Program in Material Science & Engineering, [‡]Department of Entomology, [§]Department of Veterinary Integrated Biosciences, [⊥]Department of Veterinary Physiology & Pharmacology, Texas A&M University, College Station, Texas 77843, United States

ABSTRACT: Every day, people and animals contract debilitating and life threatening diseases due to bites from infected flies, ticks, and mosquitoes. The current methods utilized to fight against these diseases are only partially effective or safe for humans and animals. When it comes to insect vector control, a conceptual paradigm shift is urgently needed. This work proposes a novel synthetic scheme to produce a nanoparticle-pesticide core–shell conjugate to be used as an active agent against arthropod vectors, such as mosquitoes. As a proof of concept, we conjugated nanosilver to the pyrethroid pesticide deltamethrin. First, electron microscopy and Fourier transform infrared spectroscopy verified the presence of a 15 nm nanosilver core surrounded by deltamethrin. Second, when the conjugate was exposed to mosquitoes for a 24 h bioassay, mortality was observed at 9×10^{-4} M. Silver was detected in the hemolymph of mosquitoes exposed to the conjugate. We concluded that the newly developed nanoconjugate did not inactivate the primary function of the pesticide and was effective in killing mosquitoes at low concentrations. These results demonstrate the potential to use nanoparticle surfaces to kill insects, specifically vectors of human pathogens.

KEYWORDS: nanoparticles, pesticides, vector control, mosquito mortality, mosquito knockdown, deltamethrin



INTRODUCTION

Every day, people and animals contract debilitating and life threatening diseases due to bites from infected flies, ticks, and mosquitoes. Not only do diseases such as malaria, West Nile virus, and Dengue Fever cause physical suffering but they also result in severe economic losses. Additionally, animals become reservoirs for arthropod borne diseases which increase the livestock morbidity and mortality and decreases reproductive capacity. This leads to a perpetual cycle of infectivity and loss.

When it comes to arthropod vector control, a conceptual paradigm shift is urgently needed. Strategies are being developed which aim to control vector populations by killing the larval stages. Biopesticides such as the Cry and Cyt toxins produced by the bacterium *Bacillus thuringiensis* (Bt) and insect growth regulators (IGRs) such as methoprene and novaluron are effective larvicides. Bt toxins have been incorporated into transgenic crops to combat agricultural insect pests. However, both Bt toxins and IGRs currently have limited use as sprays since they do not kill the adult stage and widespread coverage of breeding areas in remote locations is logistically challenging.^{1,2} Current chemical vector control strategies are limited to the same four classes of synthetic insecticides (organochlorine, organophosphate, pyrethroid, and carbamate) that have been used for over 30 years.³ In this period, no new chemicals or classes of insecticides have been successfully incorporated into vector control programs against adult mosquitoes. One major problem with using traditional insecticides

for vector control is that, over time, the insects develop resistance. Because insecticides either inhibit acetylcholinesterase (organophosphates and carbamates) or modulate the voltage gated sodium channels (pyrethroids and DDT), the development of resistance to one molecular target means many insecticides are rendered ineffective.

The research presented here is a first of its kind testing the efficacy of a novel nanoconjugate in a miniature biological model system. This biological model is the mosquito, an insect with an open circulatory system and a hydrophobic, porous external surface. This waxy cuticular surface has orifices ranging 0.5 to 2 μm , much larger than the nanometer size scale. The model nanoconjugate, termed pesticide encapsulated nanosilver (PENS), is only 15–20 nm in diameter. It is made of deltamethrin molecules tethered to the surface of nanosilver particles and designed to be a new tool to fight disease carrying insect vectors.

One of the most important properties of nanoparticles is their high surface area to volume ratio. For many different nanoparticle-types, this particular property results in high surface reactivity.^{4–8} Metal-based nanoparticles, such as silver, are unique because they offer the possibility of altering their surfaces in order to introduce specific functionalities for environmental applications.^{9–12}

Received: March 30, 2011

Accepted: September 28, 2011

Published: September 28, 2011

The ultimate goal of nanosilver synthesis for real world applications is to achieve nanoparticles with the following characteristics: (1) uniform size and narrow size distribution, (2) well-defined shape, (3) known chemical composition with no impurities, and (4) no aggregation or agglomeration.⁹ By utilizing a capping agent that acts as a colloidal stabilizer and enhances water suspendability, these highly desirable characteristics can be achieved for silver nanoparticles.^{13,14} In addition, because silver is an electron dense metal, the PENS nanoconjugate can be traced in vectors, in the environment, and in animals. Lastly, by employing a metal nanoparticle as the core of the conjugate, the risk of inactivating the primary function of the pesticide (e.g., deltamethrin) by forming covalent bonds is eliminated.

This work proposes a novel synthetic scheme to produce a nanoparticle-pesticide core-shell nanoconjugate to be used as an active agent against insect vectors, such as mosquitoes. Lab synthesized 15 nm stable silver nanoparticles were surface functionalized with deltamethrin as the capping agent resulting in a stable colloidal suspension. We characterized the physicochemical properties of both the pristine nanosilver particles and the pesticide encapsulated nanosilver (PENS) conjugate. These properties include size, size distribution, chemical composition, agglomeration states, and stability of particles. Two mosquito bioassays were also conducted to quantify the uptake of PENS via silver metal detection and to assess the mortality of mosquitoes. The act of tethering a synthetic organic molecule such as deltamethrin to a nanosilver core allows for effective tracking of organics in complex biological matrices such as mosquitoes. This is a paradigm-shifting technology and offers new possibilities for vector and pathogen control.

MATERIALS AND METHODS

Synthesis of Nanosilver Core Particles. Nanosilver particles were synthesized by reducing silver nitrate salt solution (AgNO_3 , 1×10^{-3} M) with 1% (w/w) sodium citrate ($\text{Na}_3\text{C}_6\text{H}_5\text{O}_7$). In a typical experiment, the AgNO_3 solution was heated to boiling with vigorous stirring; $\text{Na}_3\text{C}_6\text{H}_5\text{O}_7$ was mixed with a 30 μM tannic acid solution and heated separately.¹⁵ The citrate-tannic acid solution was added dropwise to the silver salt solution. The color of the mixture slowly turned from colorless to yellow indicating the reduction of Ag^+ ions.¹⁶ The solutions were removed from the heating mantle and allowed to cool.

Conjugation of the Nanosilver Core Particle with Deltamethrin. Deltamethrin (DM, 90 ppm (180 μM)) was then tethered to the surface of the resultant nanosilver particle suspension via a heating gradient and vigorous stirring. The color of the mixture slowly turned from yellow to orange, indicative of the surface functionalization. The suspension was monitored at 420 nm using Ultraviolet Visible spectroscopy for absorbance peaks and dynamic light scattering for size intensity peaks. The resultant aqueous suspension is the pesticide encapsulated nanosilver particle, termed PENS.

Characterization of Nanosilver and Pesticide Encapsulated Nanosilver (PENS). The resultant monodispersed nanosilver suspension was subsequently surface functionalized with deltamethrin molecules. These deltamethrin molecules also proved to be colloidal stabilizers. The size, morphology, crystallinity, absorbance, and zeta potential of the pristine nanosilver particles and the pesticide encapsulated nanosilver (PENS) particles were measured.

Transmission Electron Microscopy and Energy-Dispersive X-ray Spectroscopy. Electron microscopy grids were glow-discharged using PELCO easiGlow (Ted Pella, Inc., Redding, CA) to make the grid surface hydrophilic. One microliter of the nanosilver particle or PENS suspension was deposited onto a 400 mesh carbon grid.

Each grid was analyzed on a JEOL 2010 transmission electron microscope at an accelerating voltage of 200 kV. These grid samples were also probed for elemental analyses using energy dispersive X-ray spectroscopy.

UV-visible Absorption Spectroscopy. UV-visible absorption spectra were collected over a wavelength range of 200 to 700 nm using a Synergy Mx Multi-Mode Microplate Reader (BioTek Instruments, Inc., Winooski, VT).

Dynamic Light Scattering. The size distribution and the hydrodynamic diameter of the nanosilver particle and PENS suspension were measured using a Zeta Sizer Nano Series ZEN 3600 Spectrometer (Malvern Instruments Ltd., Malvern, Worcestershire, United Kingdom).

Particle Charge. Particle charge or zeta potential of the nanosilver particle and PENS suspension were also measured using a Zeta Sizer Nano Series ZEN 3600 Spectrometer (Malvern Instruments Ltd., Malvern, Worcestershire, United Kingdom).

Fourier Transform Infrared Spectroscopy. Solutions of DM and PENS were dried on a polished 25×2 mm ZnS disk (ClearTran, Internation Crystal Laboratories, Garfield, New Jersey) and analyzed using FTIR System 2000 and Spectrum 100 infrared spectrometers (Perkin-Elmer). Spectra were recorded in transmission mode with a resolution of 4 cm^{-1} . Thirty-two scans were collected and averaged for each spectrum.

Mosquito Bioassays. Experiments were conducted using adult female mosquitoes of *Aedes aegypti* (L.). The mosquitoes were fed with 10% glucose in distilled water. Two mosquito bioassays were conducted. First, a mosquito bioassay was conducted to evaluate the uptake of nanosilver particles in the mosquito hemolymph. Second, a mosquito bioassay to compare after exposure to DM and PENS was carried out. For both the mosquito bioassays, i.e., the hemolymph analysis and the viability tests, clear borosilicate glass vials (maximum capacity of 75 mL) were coated with 15 mLs of solutions (DM, nanosilver, or PENS) using a Roller Culture Apparatus (Wheaton Industries Inc., Millville, NJ). For the hemolymph analysis, vials were coated with high concentrations of solutions to ensure easy detection of silver uptake. For the viability tests, vials were coated with varying concentrations of DM and PENS. The roller action ensured uniform coating of suspensions on the walls of the vials. The experimenter was blinded to the treatment groups; and on the day of the experiment, 20 non blood-fed mosquitoes (5 days old) were placed into each of the coated glass vials and observed at specified intervals as described. Additionally, an uncoated vial served as the "negative control".

Mosquito Bioassay #1: Hemolymph Collection and Total Silver Content Analysis. Four clear borosilicate glass vials were used in these studies: vial 1 was uncoated, vial 2 was coated with nanosilver, vial 3 was coated with deltamethrin, and vial 4 was coated with PENS. Vials 2 and 4 were each coated with 90 ppm solutions of nanosilver (in water) or PENS (in water). The uncoated vial served as the "negative control" and a 90 ppm DM coated vial served as the "positive control". The mosquitoes were exposed to each treatment and were observed continuously for the first 4 h and the bioassay finalized at 24 h when survivorship was recorded. The experiment was repeated four times.

Mosquitoes from the bioassay described above were utilized to analyze their silver content in hemolymph. Mosquitoes from the negative control vials, vial 1 (uncoated) and vial 2 (nanosilver), were alive after 24 h (Figure 3A, C) and their hemolymph was collected at that time. The mosquitoes in the vials 3 (deltamethrin) and 4 (PENS) were observed knocked down 5 min after bioassay initiation, however, they were still moving. At 15 min from bioassay initiation, the mosquitoes were completely immobile and presumed dead. They were continuously observed for the next 4 h to determine if there was recovery from knock down, but they were scored as dead at 4 h.

All mosquitoes were then chilled on ice for 15 min after which each was carefully placed on a clean microscope slide under a dissecting

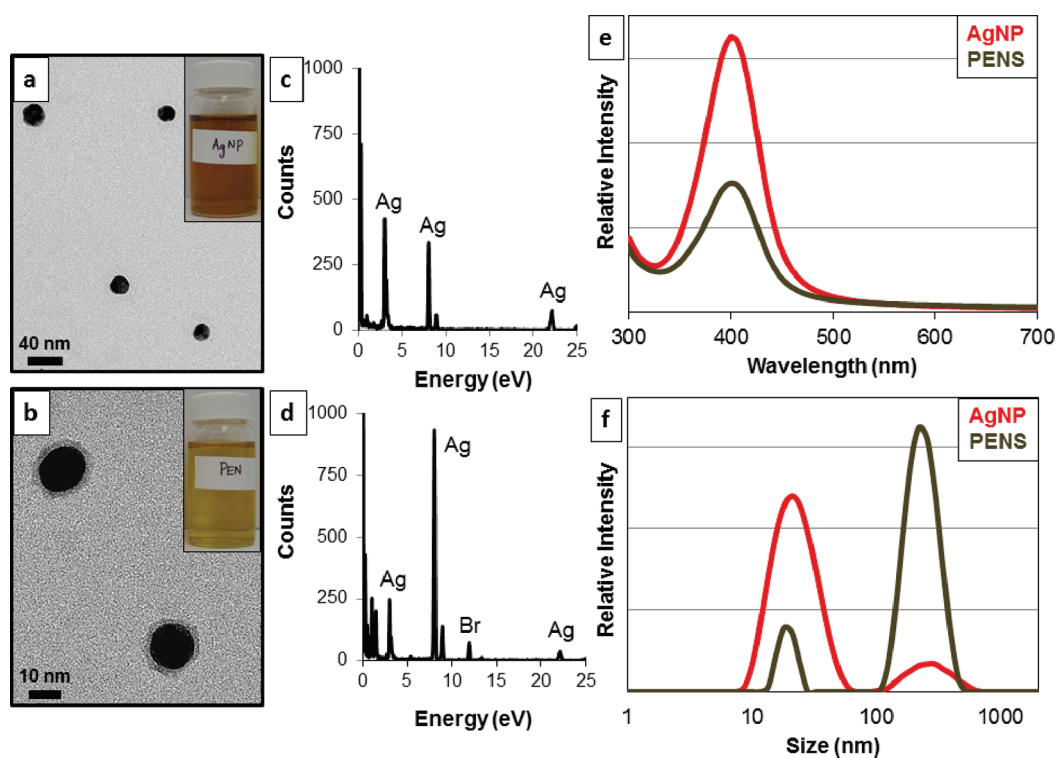


Figure 1. Synthesis and characterization of nanosilver core and PENS. (a) TEM of pristine AgNP, (b) TEM of PENS particles, (c) elemental analyses via EDS of pristine AgNP, (d) elemental analyses via EDS of PENS particles, (e) UV–vis spectra of pristine AgNP and PENS particles, and (f) dynamic light scattering spectra of pristine AgNP and PENS particles.

microscope. A 10 μL anticoagulant citrate buffered solution (98 mM NaOH, 186 mM NaCl, 1.7 mM EDTA, and 41 mM citric acid, pH 4) was then injected into the thorax using sterile glass needles (Femtotips; Eppendorf, Hamburg, Germany) connected to a FemtoJetpump (Eppendorf, Hamburg, Germany).¹⁷ After 15 min on ice, hemolymph was collected by capillary action using new Femtotips through a perforation made between the last two abdominal sclerites of each of the 20 mosquitoes exposed per treatment. Hemolymph was collected by ejecting it from the tips with the aid of the pump, and approximately 25 μL of hemolymph was obtained from each group of mosquitoes.

The collected hemolymph was then qualitatively analyzed to measure the total silver content via inductively coupled plasma-mass spectrometry (ICP-MS, Perkin-Elmer DRC 2 spectrometer, Waltham, MA). Each sample was diluted by a factor of 100 using a calibration blank solution (5% hydrochloric acid and 1% nitric acid by volume). The resultant solution was heated at 60 $^{\circ}\text{C}$ for 2 h to dissolve the residual silver particles. The citrate buffer solution was also analyzed to establish background silver concentration levels.

Mosquito Bioassay #2: Viability Tests Comparing DM and PENS. For these studies, mosquitoes were introduced into vials coated with varying concentrations of either DM or PENS and observed every hour for the first 12 h. The bioassay was finalized at 24 h when survivorship was recorded. Both knockdown and death were recorded.

Statistical Analysis. Hemolymph values are expressed as the mean plus or minus standard error of the mean ($\pm\text{SEM}$). Differences between treatment groups were analyzed by a one way analysis of variance (ANOVA) followed by posthoc testing using the Tukey-Kramer multiple comparison test. Probability values of $p < 0.05$ were considered to be statistically significant. The IBM PC programs INSTAT v3.0 and PRISM v5.0 software (GraphPad, San Diego, CA) were used to calculate and graph results.

RESULTS

Synthesis and Characterization of Nanosilver Core Particles and PENS. A primary goal of nanosilver synthesis for practical applications is to produce monodispersed nanoparticles with a well-defined shape. Therefore, careful selection of the reducing agent and stabilizer are critical steps which can be more easily controlled when the nanoparticles are synthesized “in-house”. Hence, we were able to successfully synthesize water-soluble, highly monodispersed, spherical nanosilver particles with a known chemical composition. For these experiments, sodium citrate served the dual role of both a reducing agent and a stabilizer. The well-defined nanosilver core particles were then conjugated with deltamethrin, resulting in PENS, which was also produced in water as opposed to harsh nonpolar solvents. Characterization of both the pristine nanosilver particles and the PENS conjugate are shown in detail in Figure 1.

Transmission Electron Microscopy and Energy-Dispersive X-ray Spectroscopy. Figure 1a and 1b are the transmission electron micrographs of the nanosilver and PENS respectively. Electron micrographs of pristine silver nanoparticles show 15 nm monodispersed spherical nanoparticles. Electron micrographs of the PENS clearly show a nanosilver core encircled by organic molecules. This organic molecule is the deltamethrin that was added during the conjugation reaction. Hence, these transmission electron micrographs confirm conjugation. Figure 1c and 1d show the energy-dispersive X-ray spectroscopy (EDS) spectra of pristine silver nanoparticles and PENS conjugate respectively. The EDS of nanosilver shows only silver signature peaks, whereas the EDS of PENS shows the presence of both silver and bromine. These two elements are indicative of silver particles and the

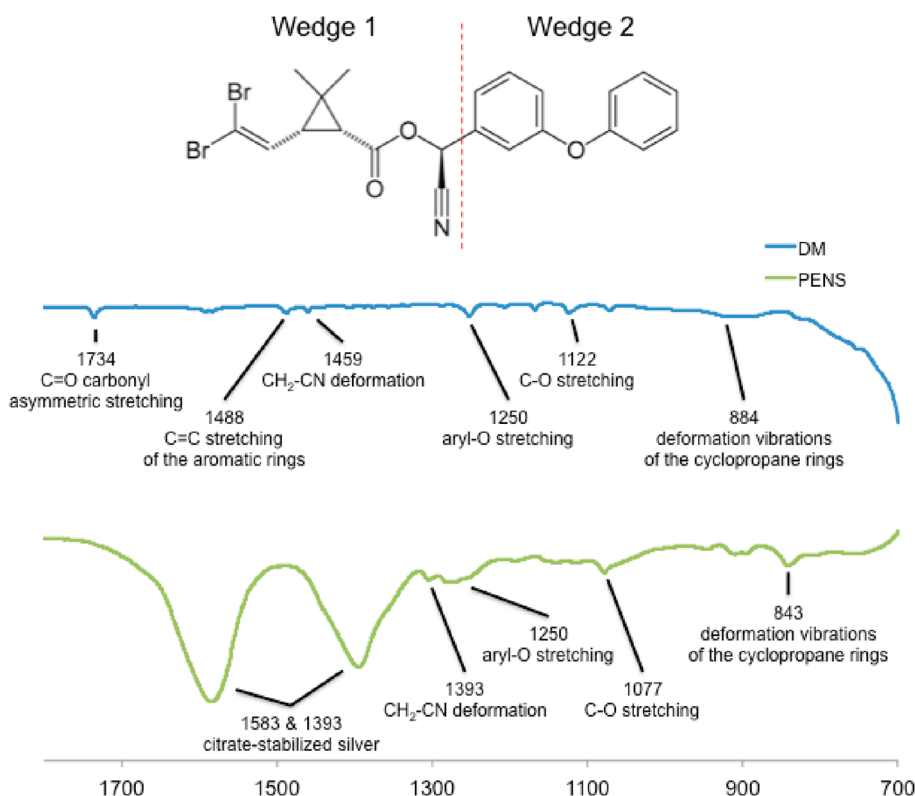


Figure 2. FTIR spectra. (Top) Structure of the deltamethrin molecule ($C_{22}H_{19}Br_2NO_3$) and the assignments of wedges as related to spectral peak assignments. (Bottom) ATR-FTIR spectrum of deltamethrin and PENS at the spectral signature region between 1800 and 600 cm^{-1} .

deltamethrin ($C_{22}H_{19}Br_2NO_3$). These results further confirm the conjugation.

UV–Visible Absorption Spectroscopy. Figure 1e shows the measurements from the UV–visible absorption spectroscopy. During the synthesis of nanosilver, the solution mixture turned from colorless to yellow (Figure 1a inset). This color change is indicative of the reduction of Ag^+ ions as revealed by the peak at 420 nm . On conjugating deltamethrin to the nanosilver core, the color of the solution mixture changed once again from yellow to orange, indicative of the surface functionalization and successful conjugation (Figure 1b inset).¹⁸ It is important to note that the overall spectral shape of the plasmon absorption remained the same for both pristine nanosilver particles and PENS indicating the presence of silver in both suspensions. The reduced peak for the PENS is indicative of the conjugation of a deltamethrin corona onto the nanosilver core.

Dynamic Light Scattering. Figure 1f shows the sizing data from the dynamic light scattering spectra. A shift in the hydrodynamic diameter from pristine nanosilver particles (AgNP) to PENS particles is seen. Both samples exhibit a bimodal size peak at ~ 20 and $\sim 200\text{ nm}$. However, the AgNP sample has a larger portion of its size population at $\sim 20\text{ nm}$ and the PENS particle sample has a larger portion of its size population at $\sim 200\text{ nm}$. These results suggest that PENS particles have a larger hydrodynamic radius and a higher aggregation potential when compared to pristine AgNP indicating the attachment of deltamethrin molecules to the nanosilver core.

Particle Charge. The overall charge that the particle acquires in a particular medium can be determined by measuring the zeta potential of the suspension. The resulting repulsive force can be used to predict the colloidal stability and agglomeration state of

nanoparticles. Particles with a large positive or negative zeta potential repel each other leading to a nonaggregated solution with high stability. Conversely, low zeta potential values result in the tendency of nanoparticles to flocculate, or coagulate loosely thereby causing agglomeration.¹⁹ The zeta potential of pristine silver and PENS were found to be around -40 mV , verifying that both the nanosilver and PENS particles were charged and stable. A high zeta potential value of -40 mV also suggests that both the nanosilver particles and PENS particles are not likely to aggregate. In addition, the size vs intensity peaks for pristine silver were around 15 nm (in accordance with electron micrographs), but the analysis of PENS shifted the spectra to a larger size range, again indicative of the deltamethrin being coated to the nanosilver core.

Fourier Transform Infrared Spectroscopy. Figure 2 shows the ATR-FTIR spectrum of DM and PENS deposited as a thin film on the ZnS disk. The molecule of deltamethrin can be divided into two characteristic parts - Wedge 1 and Wedge 2 as shown in Figure 2. Wedge 1 is the proposed “active site” of the molecule that aids in conjugation because it contains ester groups (CO), the cyanide group (CN), active dimethyl groups (CH_3) and electronegative Br atoms.²⁰ Thus, in the vicinity of interacting atoms such as a nanosilver core, Wedge 1 offers a relatively flexible structure thereby permitting the reactive CO, CN, CH_3 or the Br groups to aid conjugation.^{21,22} Wedge 2, on the other hand, is relatively rigid and provides support for such interaction to occur.^{21,22}

The ATR-FTIR spectrum shown for deltamethrin includes only the fingerprint region between 1800 and 600 cm^{-1} . In this region, the main absorption bands of deltamethrin are assigned to the C=O carbonyl asymmetric stretching ($\nu = 1734\text{ cm}^{-1}$),

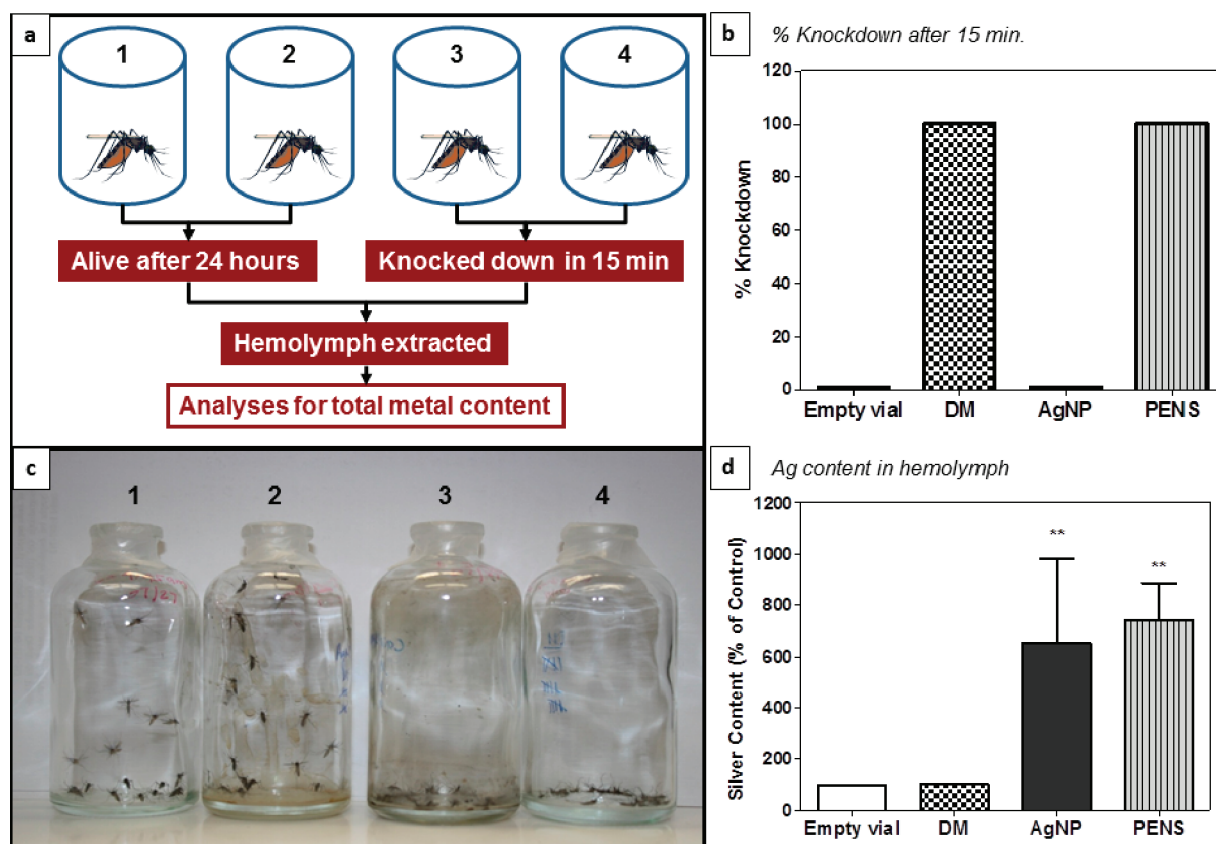


Figure 3. Effects on mosquitoes. (a) Schematic diagram of mosquito bioassay, (b) percentage knock down in vials after 15 min of exposure (vial 1 was the “negative” control (uncoated); vial 2 was coated with 90 ppm nanosilver particles; vial 3 was the “positive” control (coated with 90 ppm DM); and vial 4 was coated with 90 ppm PENS); and (d) ICP-MS analyses of total silver content in mosquito hemolymph.

C=C stretching of the aromatic rings ($\nu = 1488 \text{ cm}^{-1}$), CH_2 deformation in R- CH_2 -CN structure ($\nu = 1459 \text{ cm}^{-1}$) and the deformation vibrations of the cyclopropane rings ($\nu = 884 \text{ cm}^{-1}$). The band represented at 1122 cm^{-1} can be related to the C-O stretching of the cyanate group (-O-CN).^{23–25} It is interesting to note a clear shift in these bands for the PENS spectra. This shift in the bands indicates that the reactive groups such as CO, CN and CH_3 of the deltamethrin molecule permit interaction with other molecules in its vicinity. Since the nanoconjugate PENS was created by tethering deltamethrin molecules to a nanosilver core, this shift in the bands for PENS can be attributed to the interaction of the CO, CN and CH_3 groups of the deltamethrin with the nanosilver particle core. Furthermore, the band observed at 1250 cm^{-1} (for both DM and PENS) can be assigned to the aryl-O of diphenyl ether which involves aryl-O stretching, out-of-phase C-O-C stretching and ring vibrations. This band corresponds to rigid portion or Wedge 2 of the schematic which does not participate in bonding.^{21–25} Additionally, the band at 922 cm^{-1} for deltamethrin was assigned to the asymmetric wagging vibrations of the terminal (C=C)- Br_2 group.^{23–25} Stretching characteristic peaks of carboxylate C=O were found in 1583 cm^{-1} (asymmetry flex vibration of C=O) and 1393 cm^{-1} in the PENS spectra. These two bands confirm the presence of the nanosilver particles in the PENS sample.²⁶ Specifically, these carboxylate peaks are indicative of citrate-stabilized nanosilver particles. These results clearly show the interaction of the deltamethrin molecule with the nanosilver particles and further confirm conjugation in PENS. Taken together,

these characterization techniques confirm the presence of 15 nm stable nanosilver and the conjugation of deltamethrin to the nanosilver core.

Mosquito Bioassay #1: Hemolymph Collection and Total Silver Content Analysis. Figure 3 shows the results from the first mosquito bioassay, i.e., hemolymph collection and evaluation of total silver content. The mosquito bioassay was performed in coated vials: vial 1 was the “negative” control (uncoated); vial 2 was coated with 90 ppm nanosilver particles; vial 3 was the “positive” control (coated with 90 ppm DM), and vial 4 was coated with PENS (90 ppm DM and 90 ppm nanosilver particles) (Figure 3a). All mosquitoes in vials 3 and 4 were completely knocked down within 15 min of exposure; the mosquitoes in vial 2 were alive and had a 10% knockdown (i.e., only 2 out of the 20 exposed mosquitoes were knocked down); and the mosquitoes in vial 1 survived through the 24 h exposure time period (Figure 3b, c).

ICP-MS analysis revealed that the mosquitoes exposed to the uncoated “negative” control vial and the DM coated vial had virtually undetectable levels of silver (0.04 ng and 0.041 ng of silver, respectively). Therefore, the silver concentration in mosquitoes from the uncoated vials was set at 100% and the levels of Ag from mosquitoes exposed to DM, nanosilver and PENS were compared to the control. Hemolymph collected from mosquitoes in the nanosilver and PENS coated vials had silver levels that were higher than those of controls or those in the DM coated vial by a factor of 6 and 7, respectively ($p < 0.01$). The citrate buffer solution was also analyzed for total silver content. No significant amount of silver was detected. Thus, these results show that

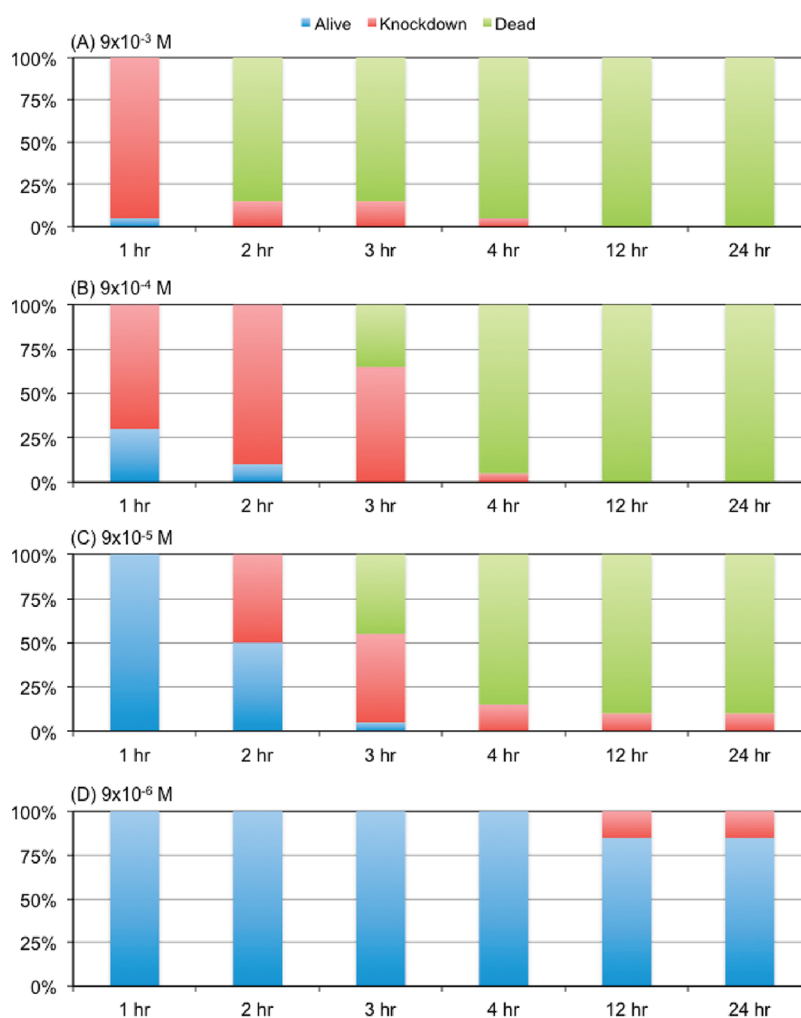


Figure 4. Effects of DM in the mosquito bioassay over time and dose. The blue bars represent mosquitoes that remained alive, the red bars represent the mosquitoes that were knocked down, and the green bars represent the mosquitoes that were scored as dead. Data are represented at the following time points: 1, 2, 3, 4, 12, and 24 h. The doses used in the bioassay were: (a) 9×10^{-3} ppm, (b) 9×10^{-4} ppm, (c) 9×10^{-5} ppm, and (d) 9×10^{-6} ppm of deltamethrin.

tethering a synthetic organic molecule to a nanosilver particle core enabled the detection of silver metal and facilitated the uptake of the pesticide into the mosquito hemolymph (Figure 3d).

In an effort to evaluate the magnitude of exogenous silver potentially introduced via the mosquito hemolymph extraction procedure, we compared the number of silver nanoparticles in the collected hemolymph to the maximum number of silver particles possibly on the surface of the femtotip (i.e., mosquito injection needle) during collection. The following reasoning was used: transmission electron micrographs verified the spherical and monodispersed nature of silver nanoparticles and confirmed the size as 15 nm (Figure 1a). On the basis of this size, the total silver content measured from ICP-MS (2.11 ng) and the density of metallic silver (10.5 g/cm^3), the number of nanosilver particles in the collected hemolymph from 20 mosquitoes was calculated as 1.14×10^8 .²⁷ Therefore, the average number of particles per mosquito was 5.76×10^6 .

The ratio of the cross-sectional area of the femtotip to that of nanosilver particles yields the maximum number of particles that are potentially on the tip of the needle as it is injected into the mosquito. This ratio was calculated to be roughly 1.11×10^3 . Hence, the amount of nanosilver particles measured from ICP-MS analysis (5.76×10^6) is more than 3 orders of magnitude

higher than the amount of silver potentially introduced to hemolymph via needle puncture (1.11×10^3). These two calculations confirm that the silver content measured via ICP-MS was indeed from the collected hemolymph and not due to exogenous silver introduced during sample collection.

Mosquito Bioassay #2: Viability Tests Comparing DM and PENS. Figures 4 and 5 show the effects of DM or PENS on mosquito viability over time and dose, respectively. Mosquitoes that remained alive are represented by the blue bars, mosquitoes that were knocked down are represented by the red bars, and the green bars represent the mosquitoes that were scored as dead. Mosquito viability (i.e., % alive, % knock down and % dead) was recorded every hour for the first 12 h and again at 24 h when the bioassay was finalized. The figures show the mosquito viability at the 1, 2, 3, 4, 12 and 24 h time points (data from hours 5–11 not shown). The doses used in the bioassay were (a) 9×10^{-3} ppm, (b) 9×10^{-4} ppm, (c) 9×10^{-5} ppm, and (d) 9×10^{-6} ppm of DM or PENS.

The results from this mosquito bioassay show that mosquitoes exposed to both DM and PENS at 9×10^{-3} ppm resulted in 100% death after 24 h. (Figures 4a and 5a, respectively). Four hours of mosquito exposure to 9×10^{-4} ppm DM resulted in 5% knockdown and 95% death; while 4 h of mosquito exposure to

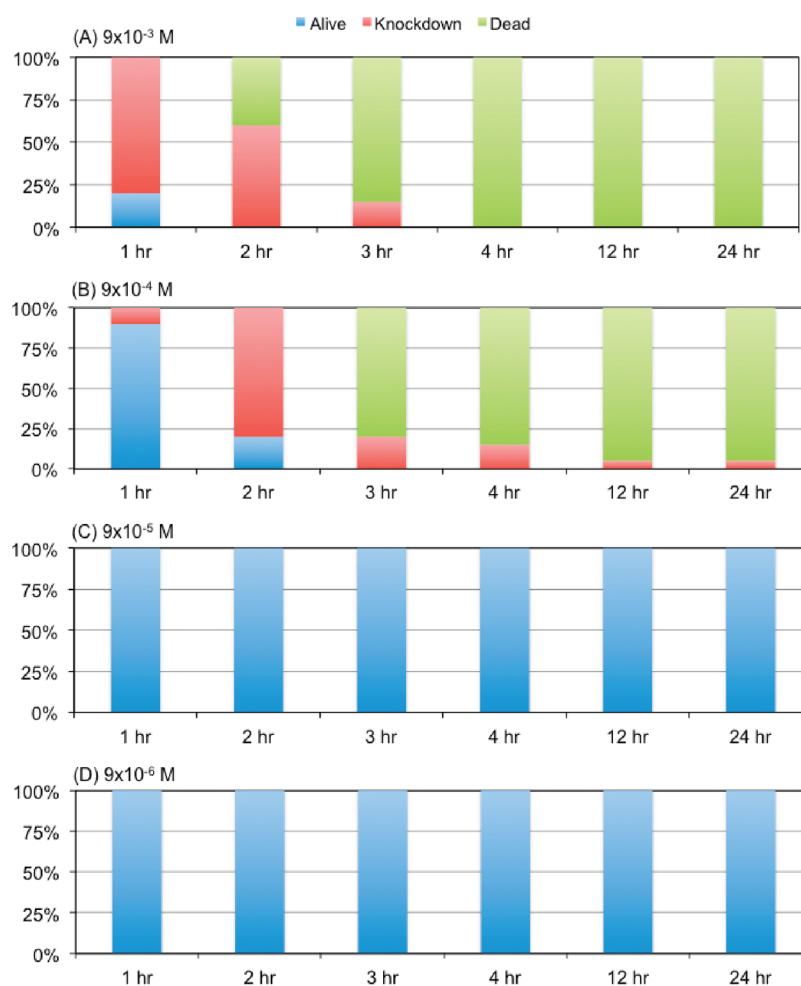


Figure 5. Effects of PENS in the mosquito bioassay over time and dose. The blue bars represent mosquitoes that remained alive, the red bars represent the mosquitoes that were knocked down, and the green bars represent the mosquitoes that were scored as dead. Data are represented at the following time points: 1, 2, 3, 4, 12, and 24 h. The doses used in the bioassay were: (a) 9×10^{-3} ppm, (b) 9×10^{-4} ppm, (c) 9×10^{-5} ppm, and (d) 9×10^{-6} ppm of PENS.

9×10^{-4} ppm PENS resulted in 15% knockdown and 85% death. At this concentration, 100% mosquito death was observed in DM vial while 95% death (with 5% knockdown) was observed after PENS exposure at the end of the 24 h period (Figures 4b and 5b). These results prove the effectiveness of the nanoconjugate in comparison to DM over time and dose.

Exposure to 9×10^{-5} ppm DM resulted in 90% mosquito death (Figure 4c); however, exposure to the PENS had no effect at this concentration (Figure 5c). The mosquitoes exposed to 9×10^{-6} ppm DM had a 15% knockdown rate with 85% staying alive (Figure 4d), whereas the mosquitoes exposed to 9×10^{-6} ppm PENS had a 100% survival rate through the 24 h exposure time period (Figure 5d). All the mosquitoes survived the entire 24 h period in the uncoated “negative control” vial (data not shown).

Hence, both PENS and deltamethrin were shown to be completely effective after 24 h of exposure to 9×10^{-3} ppm. Additionally, even though exposure to the DM resulted in 100% mosquito mortality at the 9×10^{-4} ppm concentration, the PENS exposure also resulted in 95% mosquito death and the remaining 5% were knocked down proving its effectiveness. These results show that the newly developed nanoconjugate PENS did not inactivate the primary function of the pesticide and was able to kill mosquitoes even at low concentrations.

DISCUSSION

The research presented here showcases the conjugation of monodispersed stable silver nanoparticles to the insecticide deltamethrin. It also explores the possibilities of using this newly created and effective pesticide encapsulated nanosilver (PENS) in the fight against disease carrying insects. Effective insect vector control is essential to prevention of vector-borne infectious diseases. Every day, flies, ticks, and mosquitoes infect humans and animals around the world with life threatening pathogens causative of diseases for which there are currently no vaccines or effective treatments. Therefore, alternate methods to combat infectious diseases are needed.

Current vector control strategies that target the adult insect or arthropod are limited to the same four classes of synthetic insecticides (organochlorine, organophosphate, pyrethroid, and carbamate) that have been used for over 30 years.²⁸ Introduction of insect growth regulators (IGRs) such as methoprene and novaluron as well as biopesticides such as the Cry and Cyt toxins produced by the bacterium *Bacillus thuringiensis* (Bt) have been shown to be effective larvicides. Bt toxins have been incorporated into transgenic crops to combat agricultural insect pests. However, both Bt toxins and IGRs currently have limited use as

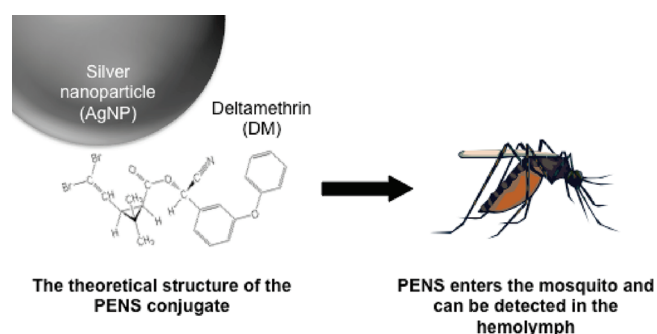


Figure 6. Overall big picture. Tethering a synthetic organic molecule to a nanosilver particle core allowed for the detection of silver metal in the mosquito hemolymph. Furthermore, the newly developed nanoconjugate did not inactivate the primary function of the pesticide and was effective in killing mosquitoes even at low concentrations.

sprays because they do not kill the adult stage and widespread coverage of breeding areas in remote locations is logistically challenging.¹ Therefore, the development of new and/or improved vector control strategies is paramount in the fight against the irrepressible spread of disease.

Many countries continue to extensively utilize the organochlorine pesticide dichlorodiphenyltrichloroethane, better known as DDT, as well as the pyrethroid pesticide deltamethrin to control mosquitoes that carry malaria.¹⁹ Even though the pyrethroids are safer than many of the other insecticides, they are neurotoxic to people, and human exposure needs to be effectively and accurately monitored. The structural diversity of the synthetic pyrethroids presents a challenge for the development and analysis of human exposure biomarkers.²⁹ Another factor complicating biomonitoring of pyrethroids is that many of the metabolites are nonspecific and are derived from the breakdown of multiple pyrethroids. Only cyfluthrin and deltamethrin yield compound specific metabolites.²⁹ However, several of the common metabolites (specific and nonspecific) also occur naturally in the environment due to microbial transformation and photolysis.³⁰ Therefore, measurement of urinary metabolites may not accurately depict pyrethroid exposure. The successful conjugation of a pesticide to a nanoparticle surface allows for effective tracking of organics in complex biological matrices. The presence of noble metals in biological fluids and other complex matrices allows for ease in detection of organometallic substances, such as PENS describes herein. Analytical methods such as mass spectroscopy, emission spectroscopy, and electron microscopy are all better suited to detect and characterize biological substances that contain elements of high electron density, such as elemental or particulate silver.

When conjugating an organic molecule to the surface of a nanoparticle, an “active site” of the molecule must be identified. In this case, deltamethrin is conjugated to the surface of a silver nanoparticle. On the basis of the evidence provided by the FTIR spectroscopy studies, wedge 1 (which contains an ester group, a cyanide group, dimethyl groups, and bromine atoms) is the “active site”. Further evidence is observed in the transmission electron micrographs showing pristine nanosilver particles before conjugation and an organic corona surrounding the nanosilver particles after conjugation with deltamethrin. When considering the effects of the PENS conjugate to mosquitoes, the bioassay resulted in mosquito knockdown and subsequent death. PENS was comparable to deltamethrin in killing mosquitoes

at a low concentration (9×10^{-4}). Measurable levels of nanosilver particles were detected in mosquito hemolymph following exposure to either the silver particles (650 ppm) or to PENS (600 ppm). Even though deltamethrin resulted in mosquito mortality at 9×10^{-5} concentrations while PENS did not, we have clearly demonstrated that the conjugation process does not inactivate the insecticide.

In conclusion, tethering a synthetic organic molecule to an engineered metal-based nanoparticle allows for the detection of the metal conjugate in complex matrices, such as mosquito hemolymph (see Figure 6). The novel synthetic scheme, material characterization techniques, and in vivo mosquito bioassays described here is a refreshing concept for the exploitation of a core–shell nanoconjugate that can be used as an active agent against insect vectors. By simply altering the chemistry of the synthesis scheme, we describe new possibilities of creating several nanoparticle–pesticide core–shell conjugate models that can be tested in other biological systems. This example of a nanoparticle-based technology will have a significant impact on both basic understanding of synthesis, characterization, and toxicology as well as having an impact in the application of such technologies toward vector control.

AUTHOR INFORMATION

Corresponding Author

*Fax: 1-979-862-4929 (C.M.S.); 1-979-862-2864 (M.H.P.).
E-mail: csayes@cvm.tamu.edu (C.M.S.); mpine@cvm.tamu.edu (M.H.P.).

ACKNOWLEDGMENT

We thank Drs. Hansoo Kim and J. Michael Berg for assistance with collecting the electron micrographs. The authors thank the Department of Veterinary Physiology & Pharmacology, Department of Veterinary Integrated Biosciences, The DuPont Company, the Texas AgriLife Vector-Borne Disease Research Program, and the CVM Office of the Associate Dean for Graduate Studies & Research for financial support.

REFERENCES

- (1) Bravo, A.; Likitvivanavong, S.; Gill, S. S.; Soberon, M. *Insect Biochem. Mol. Biol.* **2011**, *41* (7), 423–431.
- (2) Elango, G.; Rahuman, A. A.; Kamaraj, C.; Bagavan, A.; Zahir, A. A. *Parasitol. Res.* **2011**, *108* (6), 1437–1445.
- (3) Zaim, M.; Guillet, P. *Trends Parasitol.* **2002**, *18*, 161–163.
- (4) Gan, X.; Liu, T.; Zhong, J.; Liu, X. J.; Li, G. X. *Chembiochem* **2004**, *5* (12), 1686–1691.
- (5) Hamal, D. B.; Klabunde, K. J. *J. Colloid Interface Sci.* **2007**, *311* (2), 514–522.
- (6) Sylvestre, J. P.; Poulin, S.; Kabashin, A. V.; Sacher, E.; Meunier, M.; Luong, J. H. T. *J. Phys. Chem. B* **2004**, *108* (43), 16864–16869.
- (7) Yang, M. X.; Gracias, D. H.; Jacobs, P. W.; Somorjai, G. A. *Langmuir* **1998**, *14* (6), 1458–1464.
- (8) Rezaei-Zarchi, S.; Saboury, A. A.; Norouzi, P.; Hong, J.; Ahmadian, S.; Ganjali, M. R.; Moosavi-Movahedi, A. A.; Moghaddam, A. B.; Javed, A. *J. Appl. Electrochem.* **2007**, *37* (9), 1021–1026.
- (9) Ju-Nam, Y.; Lead, J. R. *Sci. Total Environ.* **2008**, *400* (1–3), 396–414.
- (10) Schmid, G.; Corain, B. *Eur. J. Inorg. Chem.* **2003**, *17*, 3081–98.
- (11) Brust, M.; Kiely, C. J. *Colloids Surf., A* **2002**, *202*, 175–86.
- (12) Haick, H. *J. Phys. D: Appl. Phys.* **2007**, *40*, 7173–86.
- (13) Poole, C. P.; Owens, F. J. *Introduction to Nanotechnology*; Wiley-Interscience: Hoboken, NJ, 2003.

- (14) Rotello, V. M. *Nanoparticles: Building Blocks for Nanotechnology*, 1st ed.; Springer: New York, 2003.
- (15) Dadosh, T. *Mater. Lett.* **2009**, *63* (26), 2236–2238.
- (16) Pillai, Z. S.; Kamat, P. V. *J. Phys. Chem. B* **2004**, *108* (3), 945–951.
- (17) Castillo, J. C.; Robertson, A. E.; Strand, M. R. *Insect Biochem. Mol. Biol.* **2006**, *36* (12), 891–903.
- (18) Lee, P. C.; Meisel, D. *J. Phys. Chem.* **1982**, *86* (17), 3391–3395.
- (19) Wang, L.; Zhao, W.; Tan, W. *Nano Res.* **2008**, *1* (2), 99–99–115.
- (20) Saxena, P. N.; Chauhan, L. K. S.; Gupta, S. K. *Toxicology* **2005**, *216* (2–3), 244–252.
- (21) Owen, J. D. *J. Chem. Soc., Perkin Trans. 1* **1975**, No. 19, 1865–1868.
- (22) Owen, J. D. *Acta Crystallogr., Sect. B* **1981**, *37* (JUN), 1311–1314.
- (23) Segal-Rosenheimer, M.; Dubowski, Y. *J. Phys. Chem. C* **2007**, *111* (31), 11682–11691.
- (24) Armenta, S.; Quintas, G.; Garrigues, S.; de la Guardia, M. *TrAC, Trends Anal. Chem.* **2005**, *24* (8), 772–781.
- (25) Lin-Vien, D.; Cothup, N. B.; Fateley, W. G. Grasselli, J. G. *The Handbook of Infrared and Raman Characteristic Frequencies of Organic Molecules*; Academic Press: New York, 1991
- (26) Mo, L. X.; Li, L. H.; Li, Y. L.; Li, Z. X.; Wang, M. *Surf. Eng.* **2008**, Vol. 373–374, 698–701.
- (27) Li, X. A.; Lenhart, J. J.; Walker, H. W. *Langmuir* **2010**, *26* (22), 16690–16698.
- (28) Zaim, M.; Guillet, P. *Trends Parasitol.* **2002**, *18* (4), 161–163.
- (29) Sudakin, D. *Clin. Toxicol.* **2006**, *44*, 31–37.
- (30) Erstfeld, K. M. *Chemosphere* **1999**, *39*, 1737–1769.